PORE CHARACTERIZATION OF RESERVOIR ROCKS BY INTEGRATING SCAL AND PETROGRAPHY

Xiangmin Zhang and Albert Hebing
PanTerra Geoconsultants B. V. (x.zhang@panterra.nl)

This paper was prepared for presentation at the International Symposium of the Society of Core Analysts held in Avignon, France, 8-11 September, 2014

ABSTRACT

Pores of reservoir rock control its petrophysical and flow properties and are of importance for hydrocarbon exploration and development. We present an integrated study on pore characterization on several typical reservoir rocks, namely glauconitic sandstone, shaly sandstone, salt-cemented sandstone and chalk using SCAL data from lab nuclear magnetic resonance (NMR), high pressure mercury injection (MICP) and by SEM and thin section. NMR T2 relaxation distributions reveal patterns similar to pore-throat size distributions obtained from the (MICP) tests carried out on the same samples. Chalk samples show narrow uni-modal pores, while the glauconitic sandstones and some shaly sandstones with pore filling kaolinite show bi-modal pore size distribution. Thin section and SEM observations show that intra-granular and inter-granular pores of glauconite, kaolinite etc. correspond to micro-pores seen in NMR T2 relaxation and MICP data. The abundance of clay indicated by petrography correlates to the amplitudes of the micropore peaks of NMR T2 relaxation and pore throat size distributions in sandstone samples. Uniform intergranular pores result from fine-grained broken coccolith grains explain the narrow mono-modal T2 relaxation and pore throat distributions in chalk. The apparent T2 relaxivities for glauconite and calcite are derived.

INTRODUCTION

Pore characteristics of reservoir rocks, which result from the geological processes of deposition and diagenesis, determine their petrophysical and flow properties. Thus characterization of pore structure of reservoir rocks is of importance for hydrocarbon exploration and development. Petrography thin section and SEM reveal the mineral composition, fabric texture which forms the frames of pores and pore geometry. SCAL analyses such as lab NMR and MICP provide quantitative measurements of the pore size and pore-throat size of reservoir rocks respectively, spanning five orders of magnitude from nano meter to millimeter. On the other hand, NMR measurement can be performed in a borehole by a wireline logging tool. Integration of NMR, MICP data and petrography helps to convert NMR T2 distributions to drainage capillary pressure curves generating continuous capillary pressure data as well as to characterize the reservoir rocks with depth.

The aims of this study are: 1) to characterize several typical reservoir rocks of chalk, glauconitic sandstones and shaly sandstones (containing kaolinite and illite clays) and micro-porosity by NMR, MICP, and petrography; 2) to derive surface relaxation of pore characteristic minerals which form well-characterized pores, for better conversion from T2 distribution to pore size distribution. Our results show that some reservoir rocks such as chalk, glauconitic sandstones and some pore filling kaolinitic sandstones can be

characterized by its T2 distributions. The chalk is a model sample for deriving T2 relaxivity for calcite as it has simpler pore structures compared to other carbonate rocks (such as limestones). The clay minerals in the shaly sandstone are the controlling factor for micro-porosity and thus irreducible water saturation.

DATA AND METHOD

Samples were plugged and trimmed from whole cores taken from various wells. The plug and the trim samples were cleaned and dried, prior to analysis. Subsequently, Klinkenberg permeability and helium porosity were measured, and then brine saturated for NMR testing. Following the 100% NMR measurement, the samples were then de-saturated by a ultra-centrifuge and NMR analysis was repeated at irreducible saturation. The corresponding trims of the plug samples were used for MICP, petrography of thin section and SEM analyses. The obtained NMR data, MICP and petrography of the same sample were integrated.

Laboratory NMR measurements were performed using a MARAN-2 NMR spectrometer at a proton resonance frequency of 2.04 MHz. T2 relaxation time was measured using CPMG pulse sequence with a waiting time of 0.1 ms and echo spacing of 300 ms. The NMR spectrometer was calibrated before each batch run for hydrogen index correction for various salinities. Sample temperature was controlled at 35 °C during NMR tests. The T2 relaxation curves were then inverted to T2 distribution. The NMR porosity and Log mean T2 were calculated for each saturated sample. NMR data of de-saturated samples were used to characterize the pore system. The T2 relaxation time is related to the pore size by (Coates et al. 1999):

$$\frac{1}{T_2} = \rho \frac{S}{V} \qquad (1)$$

where ρ is the T2 relaxivity of a mineral, S/V is the ratio of specific surface area to volume of pore. Assuming a cylinder pore geometry, S/V is related to the pore radius by S/V = 2/r.

High pressure mercury injection was performed by an Autopore-IV automated porosimeter. The test sample was placed in a specifically selected penetrometer of which the final intrusion volume to the sample was in the range of 20-80% of its stem volume. About 200 capillary pressure steps ranging from 0.5 to 60,000 psia were programmed for each test. The penetrometer and sample was first vacuum filled. Mercury was then injected into the sample in two steps, first by compressed dry air till 30 psia and then by hydraulic oil from ambient to 60,000 psia. For each capillary pressure step, mercury was injected till the desired pressure reached and 99.5% its pressure kept in the duration equilibrium time of 60 seconds. The injection volumes were measured by measuring the electrical capacitance of the silver coated penetrometer stem. The capillary pressure curve can be generated by plotting the pressures against the mercury saturations calculated by injection volumes. The pore throat size at a capillary pressure can be converted by:

$$r = \frac{2\sigma \cdot \cos\theta \cdot C}{P_c} \qquad (2)$$

where r is pore throat radius, σ is interfacial tension, θ is contact angle and Pc is capillary pressure. The pore throat distribution can be converted from the capillary curve and the mean hydraulic diameters can then be calculated in the similar way of Log T2 mean.

Microphotographs were taken by SEM on fractured sample surfaces and by optical microscopy on blue dyed thin sections. Mineral composition, microstructure, pore structures and geometry can be interpreted.

Integration of the NMR and MICP data were achieved using a similar method to that described by Marschall, et al. (1995). The NMR T2 distribution and MICP pore throat size distribution were correlated for each sample. Log mean T2 and mean hydraulic diameters were then calculated.

RESULTS AND DISCUSSION

Table 1 lists the samples with their permeability and three porosity values measured by helium gas expansion, MICP and NMR respectively. The porosity values measured in three methods are very close for the chalk samples while large differences occur in some shaly sandstones. For most of the samples, the T2 NMR distribution of fully saturated individual sample resembles its MICP pore throat size distribution.

Figure 1 shows the microphotographs of studied samples. Figure 1a is SEM image of typical chalk consisting of uniform fine grain sized calcite of broken coccoliths. Figure 1b is thin section image of glauconitic sandstone with glauconite grains in green and quartz grains in white. Figure 1c shows a sandstone with intergranular pores filled with kaolinite. Pores are in blue in Figure 1b and 1c. Figure 1d is a SEM image showing a typical pore which is filled with kaolinite clay. Figure 1e shows pore scale fibered illite structures coating the quartz grains and bridging the intergranular pore. Figure 1f is a SEM showing “sheet-shaped” grain boundary cracks between halite and quartz grains.

MICP data of the chalk samples show narrow uni-modal pore throat size distribution and the T2 relaxation show the same well-defined uni-model distributions (Figure 2). The mean hydraulic diameters and the Log mean T2 relaxation times of the chalk samples are well correlated. The derived relaxivity value for calcite is 9.29 μm/s. The porosity values measured in three methods are very close for chalk. The chalk is a model sample for deriving relaxivity data for calcite due to its simple pore structures compared to other carbonate rocks such as limestone.

The T2 relaxations of glauconitic sandstones measured at fully saturated and de-saturated states are shown in Figure 3a and 3b. The greenstone samples show distinct bi-modal pore size distributions. The MICP pore throat size distribution curves (Figure 3c) show the same pattern as the fully saturated NMR curves, i. e. a well-defined bi-modal distribution. Detailed integrated analysis of these glauconite sandstones further show that the relative amplitudes of shorter T2 peaks and smaller-sized pores from MICP were related to the abundance of glauconite grains in the sandstones. The NMR relaxations on de-saturated samples show only the shorter T2 peaks. The short T2 peaks are correlated to the smaller pores of the MICP and the apparent relaxivity of glauconite is about 5.0 μm/s. The diameters of intra-grain pores of glauconite are about 20-50 nm. Hossain et al (2012) also observed the same bi-modal T2 relaxation for glauconitic sandstones.

The sandstones with pore filled kaolinite also show bi-modal pore throat size distributions from MICP and the T2 relaxation of a similar type (Figure 4a, b, c). However, compared to glauconitic sandstones, the bi-modal distribution is less well-defined depending on the contents of the kaolinite, but also on quartz grain size and degree cementation etc. The illitic sandstones normally do not show bi-modal distributions but show ill-defined uni-modal profiles with a long and/or fat tails at the small pore side or the shorter T2 parts (Figure 4d, 4e).

SEM of the salt-cemented sample indicates the pores are basically fractures along grain boundaries (Figure 1f). The range of the T2 and pore size by MICP are the same order of magnitudes, however, the T2 distributions do not show the triple peaks of the pores as MICP do (Figure 4f), but show a broad uni-model distribution (Figure 4g). This may reflect the differences on how NMR and MICP see the fracture-type pores.

Except for the chalk and glauconitic sandstones, the observed characters presented in this paper in shaly sandstones, may not be all the same in other reservoirs. Characteristics may depend on the clay types and contents; as well as grain size and cements etc. In this study, we only dealt with the single fluid in the rocks. In reservoirs, where two or three fluid phases are present, wireline Logging NMR might see the pore characteristics differently due to presence of hydrocarbon, such as in the case of oil reservoir of chalk (Looyestijn & Steiner, 2012).

CONCLUSIONS

Integration of NMR & MICP with petrographic observations helps to characterize and understand pore systems of reservoir rocks. Chalk has pores with uni-model pore & pore throat size distributions. Chalk is a model sample for deriving relaxivity data for calcite for its simple pore structures compared to other carbonate rocks such as limestone. Glauconitic sandstones show characteristic bi-modal T2 distribution with intra-grain pores with diameters 20-50 nm. Shaly sandstones are less characteristic pores depending on grain size, cements and clay types and contents etc. Salt-cemented sandstone has sheet-shaped fracture micropores which result in broad T2 distribution.

REFERENCES

1. Marschall, D., Gardner, J.S and Mardon, D., 1995. Method for Correlating NMR Relaxometry and Mercury Injection Data. Presented at the Society of Core Analysts International Symposium, San Francisco, California, USA, 12–14 September. SCA-9511.
2. Coates, G. R., Xiao, L. Z and Prammer, M. G., 1999, NMR logging: principles and applications, Haliburton Energ`y Services, Houston.
3. Ohen, H. A., Enwere, P. M., and Kier, J., 1999, NMR relaxivity grouping or NMR facies indetification is to effective integration of core NMR data with wireline log, SCA-9942.
4. Hossain, Z., Grattoni, C A., Solymar, M and Fabricius, I. L. 2011, Petrophysical properties of greensand as predicted from NMR measurements. *Petroleum Geoscience*, Vol. 17, No. 2, p. 111-125.
5. Looyestijn, W., and Steiner, S., 2012, New approach to interpretation of NMR logs in a lower Cretaceous chalk reservoir, SPWLA 53rd Annual Logging Symposium held in Cartagena, Colombia, June 16-20, 2012.

Sample	Klink-k (mD)	He- ϕ (%)	NMR-ϕ (%)	MICP-ϕ(%)	Lithology	Pores
C1	1.48	34.9	34.8	35	Chalk	Uni-modal pores
C2	1.42	35.5	35.9	33.1	Chalk	Uni-modal pores
C3	0.42	30	30.3	29.3	Chalk	Uni-modal pores
C4	0.29	28.4	29.2	27.6	Chalk	Uni-modal pores
C5	4.2	33.6	35.1	32.4	Chalk	Uni-modal pores
S1	0.02	7.2	7.3	7.5	Glauconitic SS	Bi-modal pores
S2	1.06	14.3	13.8	13.4	Glauconitic SS	Bi-modal pores
S3	0.63	13.9	13.3	14.8	Glauconitic SS	Bi-modal pores
S4	2.93	17.4	15.4	16.7	Glauconitic SS	Bi-modal pores
S5	4.95	15.2	14.6	14.1	Glauconitic SS	Bi-modal pores
KS1	0.37	7.8	8.1	7.04	Kaolinitic SS	Bi-modal pores
KS2	11.7	14.9	14	13.4	Kaolinitic SS	Bi-modal pores
KS3	0.35	8.1	6.6	7.6	Kaolinitic SS	Bi-modal pores
KS4	1.11	8.7	8.6	7.8	Kaolinitic SS	Bi-modal pores
KS5	0.11	5.9	5.1	6.0	Kaolinitic SS	Bi-modal pores
IS1	130	16.8	15.3	17.3	Illitic SS	Uni-model with long tail
IS2	1.3	10.5	10.0	10.7	Illitic SS	Uni-model with long tail
IS3	14.7	18.2	18.6	17.4	Illitic SS	Uni-model with long tail
IS4	3.9	16.6	18.3	17.1	Illitic SS	Uni-model with long tail
IS5	1.9	14.7	14.6	15.1	Illitic SS	Uni-model with long tail
HS1	6.03	5.1	5.2	3.3	Halite-cemented SS	Grain-boundary cracks
HS2	0.08	5.0	4.8	4.5	Halite-cemented SS	Grain-boundary cracks
HS3	0.78	11.6	11.5	11.3	Halite-cemented SS	Grain-boundary cracks

Table 1. list of samples.

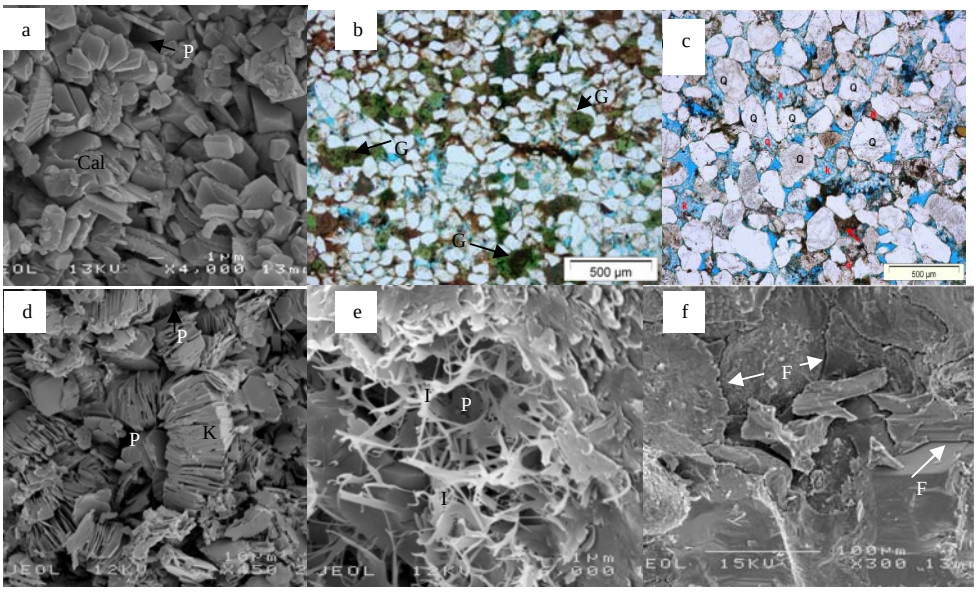

Figure 1. Microphotographs of samples by optical microscopy and SEM. P-pore, F-fracture.

Cal- calcite, G- glauconite
Q-quartz, K-kaolinite, I-illite

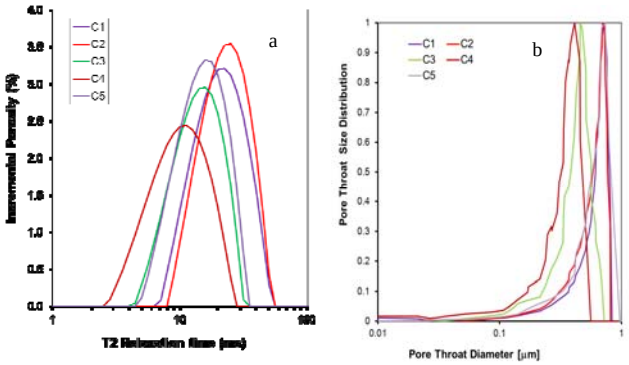

Figure 2. T2 relaxations (a) and MICP pore throat size distributions (b) of chalk samples.

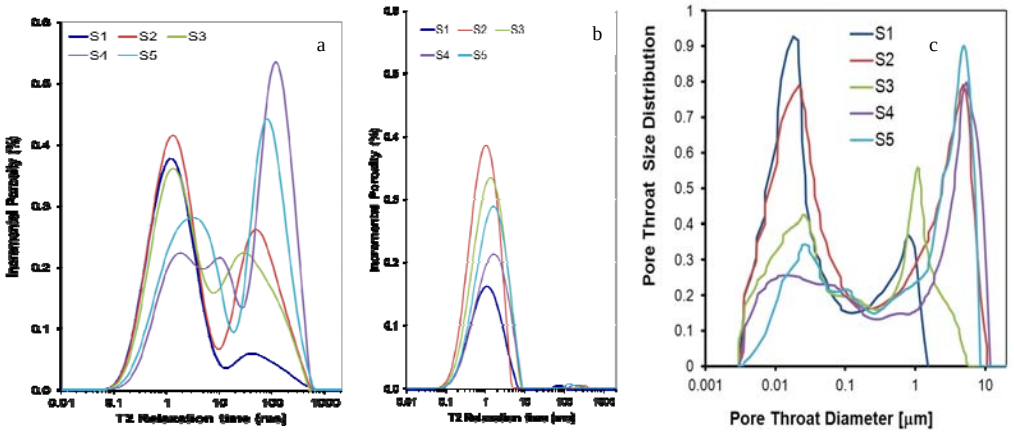

Figure 3. T2 relaxation curves of glauconitic sandstones at fully saturated states, desaturated states and Pore throat size distributions by MICP.

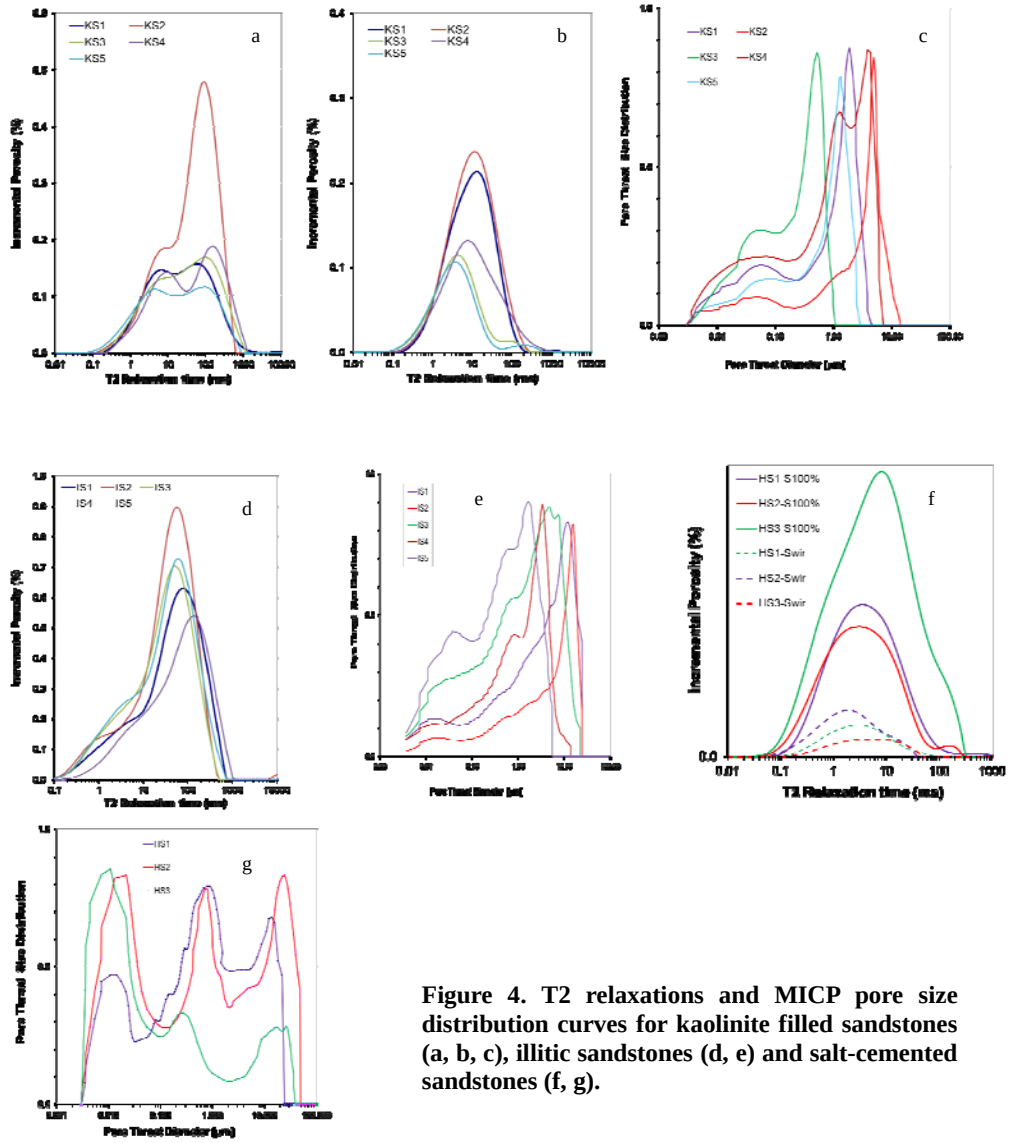

Figure 4. T2 relaxations and MICP pore size distribution curves for kaolinite filled sandstones (a, b, c), illitic sandstones (d, e) and salt-cemented sandstones (f, g).